Proceedings of the DIS'2004, Štrbské Pleso, Slovakia

THE BLACK BODY LIMIT IN DEEP INELASTIC SCATTERING

T.C. ROGERS AND M.I. STRIKMAN
Pennsylvania State University
University Park, Pennsylvania 16802, U.S.A.
E-mail: rogers@phys.psu.edu

We use information from DIS and the two gluon nucleon form factor to estimate the impact parameter amplitude of hadronic configurations in the dipole model of DIS. We demonstrate that only a small fraction of the total $\gamma^* N$ cross section at $x \sim 10^{-4}$ is due to scattering that occurs near the black body limit. We also make comparisons with other models and we point out that a quark mass of $\lesssim 100$ MeV^2 leads to a strong variation of the the t-dependence with Q^2.

1 Introduction

When one assumes that the scattering amplitude for hadron-hadron scattering is purely imaginary, unitarity implies that the total elastic cross section, $\sigma_{el}(b)$, is less than the total inelastic cross section, $\sigma_{in}(b)$, at impact parameter, b (a small real part leads to a small correction). The unitarity limit is saturated when $\sigma_{el}(b) = \sigma_{in}(b)$, which is equivalent to the condition that the profile function defined by, $\Gamma_h(s,b) \equiv \frac{1}{2is(2\pi)^2} \int d^2\vec{q} e^{i\vec{q}\cdot\vec{b}} A_{hN}(s,t)$, is equal to unity. When this situation is reached, the target is totally absorbing at impact parameter, b, and scattering is said to occur in the black body limit (BBL). See, for example, Ref. [1].

Within the dipole model of DIS, the total $\gamma^* N$ cross section is written as the convolution of the basic cross section for the interaction of the virtual photon's hadronic constituents with the square modulus of the photon wave function:

$$\sigma_{L,T}^{\gamma^* N}(Q^2, x) = \int_0^1 dz \int d^2\vec{d} \left|\psi_{L,T}(z,d)\right|^2 \hat{\sigma}_{tot}(d, x'), \tag{1}$$

where x' is a function of Q^2. We will discuss the nearness of the hadronic constituent cross sections, $\hat{\sigma}_{tot}(d, x')$, to the BBL. We use the model of McDermott, Frankfurt, Guzey, and Strikman (MFGS), discussed in Ref. [2], to interpolate between the hard and soft regimes for the total cross section. For the t-dependence, discussed in section 2, we use a model discussed in Ref. [3]. In the next section, we will demonstrate that a non-negligible fraction of the total cross section receives contributions from hadronic scattering near the BBL. In section 3, we will compare our model of the basic hadronic cross section with other models, and we will discuss the necessity of using constituent quark masses in the photon wave function.

2 Modeling the t-dependence

We use the following model for the basic hadronic amplitude:

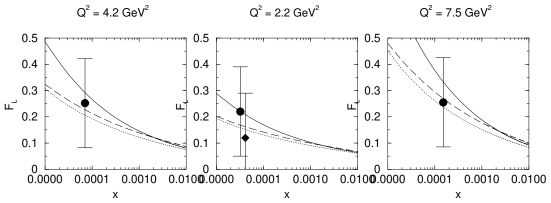

Figure 1. MFGS model prediction for F_L vs. x showing consistency with preliminary HERA data. The circular points correspond to H1 mb99(shape) and the diamond shaped point corresponds to H1 svtx00(shape) (see Ref. [4]). The dashed, solid and dotted curves correspond to the different parton distributions, CTEQ6L, CTEQ5L, and MRST98 respectively [6,7,8].

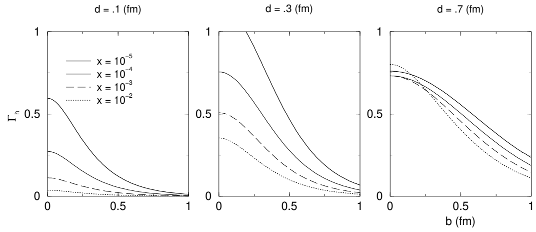

Figure 2. Samples of the profile function for different hadronic sizes.

$$A_{hN}(s,t) = is\hat{\sigma}_{tot}\frac{1}{(1-t/M^2(d^2))^2}\,\frac{1}{1-td^2/d_\pi^2 m_2^2}\,e^{\alpha' \frac{d^2 t}{d_\pi^2} \ln \frac{x_0}{x}}, \qquad (2)$$

with,

$$M^2(d^2) = \begin{cases} m_1^2 - (m_1^2 - m_0^2)\frac{d^2}{d_\pi^2}\ , & d \le d_\pi \\ m_0^2 & , \ \text{otherwise} \end{cases} . \qquad (3)$$

(See Ref. [3] for the detailed procedure.) Here, $m_1^2 \approx 1.1$ GeV^2, $m_0^2 \approx 0.7$ GeV^2 and $m_2^2 \approx 0.6$ GeV^2. The typical size of the pion is $d_\pi \approx 0.65$ fm, α' is 0.25, and $x_0 = .01$. It can be checked that this form of the amplitude reproduces the expected small size, hard behavior while yielding the phenomenologically known behavior of the larger size, soft configurations. The exponential factor in Eq. 2 takes into account scattering by soft Pomeron exchange. Figure 2 shows some samples of the resulting profile function for small and larg hadronic sizes, and Fig. 3 demonstrates that a small fraction of the total cross section, obtained from Eq. 1, is due to scattering near the BBL. We would like to stress that the MFGS model makes reasonable predictions for F_L at low Q^2 which is demonstrated in Fig. 1 which makes comparisons between the MFGS predictions and preliminary data from Ref. [4]. This parameterization is consistent with HERA data on J/Ψ [5].

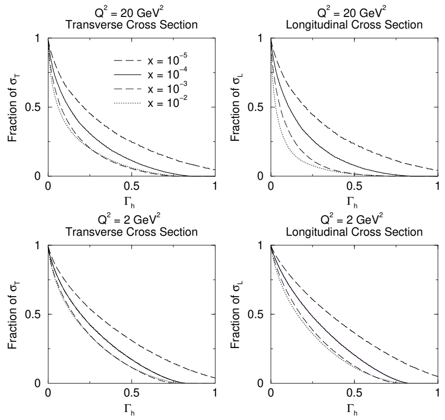

Figure 3. The fraction of the total cross section due to large values of the profile function. Note the small difference between the longitudinal and transverse cross sections. We believe this to be a numerical effect.

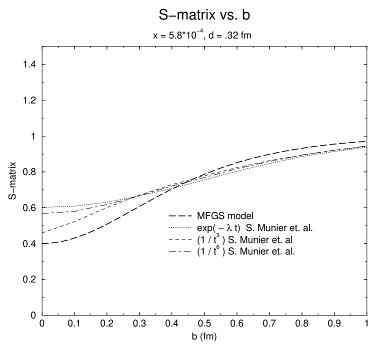

Figure 4. Consistency of the MFGS model with one using ρ meson production alone. The dotted, dashed and dot-dashed curves are taken from Ref. [9].

3 Comparisons with other models

A model similar to ours, but which only uses ρ-meson production is discussed in Ref. [9]. This model yields qualitatively similar results to what we have found [10]. A comparison between these two models is shown in Fig. 4. (Note the definition, $S(b) = 1 - \Gamma(b)$.) We would like to stress that data for ρ production is limited to kinematics where $-t \lesssim 0.6$ GeV^2 ($b \gtrsim 0.3$ fm), whereas the MFGS model is valid down to much smaller values of $-t$.

The model of Golec-Biernat and Wusthoff (GBW) [11,12], and its extension in Ref. [13], imposes exponential taming at large hadronic sizes (soft physics). In order to match the large size behavior to the perturbative, small size regime, the GBW model requires that the light quark masses remain small (0.0 to 0.14 GeV) even in the large size, nonperturbative regime. In the MFGS model, the light quark mass in

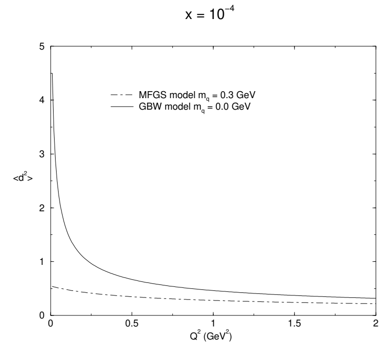

Figure 5. Average squared hadronic size for the MFGS model and the GBW model. This plot demonstrates the significant sensitivity to the quark mass at low Q^2.

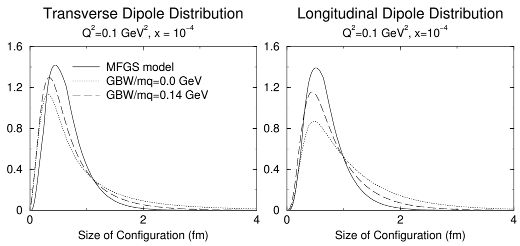

Figure 6. Normalized distribution of hadronic sizes for our model with light quark masses equal to 0.3 GeV^2 and charm mass equal to 1.5 GeV^2, compared with the saturation model with all quark masses set to zero (dotted line) and with all masses equal to 0.14 GeV^2 (dashed line).

the soft regime is fixed at a value of the order of hadronic masses (i.e., constituent quark mass). Form factors in the hard regime are naturally nearly independent of the quark mass. However, at small Q^2 the cross section becomes very sensitive to the light quark mass. This is demonstrated in Fig. 5 which shows large variation of the average hadronic size between the MFGS model and the GBW model. The small quark mass which is forced upon the model of Golec-Biernat and Wusthoff probably overestimates the contribution from large size configurations at small Q^2. Figure 6 demonstrates the large contribution from large size configurations in the model of Golec-Biernat and Wusthoff for $Q^2 = 0.1$ GeV^2. Thus, we conclude that, for an exclusive process like $\gamma^* p \to \gamma p$, and for $0 \lesssim Q^2 \lesssim .1$ GeV^2, the t-dependence in the GBW model varies strongly with Q^2.

4 Conclusion

We conclude that effects from the proximity to the BBL will be small for $x \lesssim 10^{-4}$ for $Q^2 \approx 2$ GeV^2. With the extra color factor of 9/4 that appears when we consider a gluon dipole, the interaction is closer to the BBL. This is consistent with diffractive HERA data. We also note that our model has qualitative consistency with other dipole models based on different methods. We have stressed that special care must be taken in choosing the quark masses at small values of Q^2. We also wish to point out that lattice QCD calculations and approximations from instanton models support the use of large light quark masses in the small Q^2 regime. (See Ref. [14] for an overview of nonperturbative calculations.)

Acknowledgements

We would like to thank J. Collins, L. Frankfurt, A. Mueller, C. Weiss, M. Diehl, and X. Zu for useful discussions.

References

1. V. N. Gribov, Sov. J. Nucl. Phys. **9**, 369 (1969) [Yad. Fiz. **9**, 640 (1969)]. V. N. Gribov, Sov. Phys. JETP **29**, 483 (1969) [Zh. Eksp. Teor. Fiz. **56**, 892 (1969)].
2. M. McDermott, L. Frankfurt, V. Guzey and M. Strikman, Eur. Phys. J. C **16**, 641 (2000) [arXiv:hep-ph/9912547].
3. T. Rogers, V. Guzey, M. Strikman and X. Zu, Phys. Rev. D **69**, 074011 (2004) [arXiv:hep-ph/0309099].
4. H1prelim-03-043 E. Lobodzinska
5. L. Frankfurt, M. McDermott and M. Strikman, JHEP **0103**, 045 (2001) [arXiv:hep-ph/0009086].
6. H. L. Lai *et al.* [CTEQ Collaboration], Eur. Phys. J. C **12**, 375 (2000) [arXiv:hep-ph/9903282].
7. J. Pumplin, D. R. Stump, J. Huston, H. L. Lai, P. Nadolsky and W. K. Tung, JHEP **0207**, 012 (2002) [arXiv:hep-ph/0201195].
8. A. D. Martin, R. G. Roberts, W. J. Stirling and R. S. Thorne, Eur. Phys. J. C **4**, 463 (1998) [arXiv:hep-ph/9803445].
9. S. Munier, A. M. Stasto and A. H. Mueller, Nucl. Phys. B **603**, 427 (2001) [arXiv:hep-ph/0102291].
10. We thank A. Mueller for discussions on how to optimally compare results of the two analyses.
11. K. Golec-Biernat and M. Wusthoff, Phys. Rev. D **59**, 014017 (1999) [arXiv:hep-ph/9807513].
12. K. Golec-Biernat and M. Wusthoff, Phys. Rev. D **60**, 114023 (1999) [arXiv:hep-ph/9903358].
13. J. Bartels, K. Golec-Biernat and H. Kowalski, Phys. Rev. D **66**, 014001 (2002) [arXiv:hep-ph/0203258].
14. D. Diakonov, Prog. Part. Nucl. Phys. **51**, 173 (2003) [arXiv:hep-ph/0212026].